Calcif Tissue Int (1994) 54:106–112

Calcified
Tissue
International

Fractal Signature Analysis of Macroradiographs Measures Trabecular Organization in Lumbar Vertebrae of Postmenopausal Women

J. C. Buckland-Wright,[1] J. A. Lynch,[1] J. Rymer,[2] I. Fogelman[3]

[1]Division of Anatomy and Cell Biology, United Medical and Dental Schools of Guy's and St Thomas's Hospitals, London Bridge, London SE1 9RT, U.K.
[2]Department of Obstetrics and Gynaecology, United Medical and Dental Schools of Guy's and St. Thomas's Hospitals, London Bridge, London SEI 9RT, U.K.
[3]Department of Nuclear Medicine, United Medical and Dental Schools of Guy's and St. Thomas's Hospitals, London Bridge, London SEI 9RT, U.K.

Received: 17 June 1993 / Accepted: 10 August 1993

Abstract. High definition macroradiography was used to provide an image of the detailed structural organization of the cancellous bone in human lumbar vertebrae. The fractal signature analysis (FSA) method was used to quantify the horizontal and vertical trabecular organization recorded within the image. Comparison of the FSA of the postero-anterior and lateral macroradiographs in postmortem lumbar vertebrae showed that neither the superimposition of the neural arch nor the radiographic angle affected the trabecular measurement within the vertebral body. FSA analysis of the trabecular structure measured from the macroradiographs of lumbar vertebrae in two groups of postmenopausal women, with high and low bone mineral density (BMD), showed that the large vertical trabecular structures correlated with the women's body weight ($P < 0.01$–0.03) and body mass index ($P < 0.005$–0.05), the fine horizontal structures correlated with the women's age ($P < 0.005$–0.05), and fine vertical trabecular structures were significantly greater ($P < 0.005$–0.05) in the low compared with the high BMD group.

Key words: Postmenopausal women — Lumbar vertebrae — Trabecular organization — Macroradiography — Fractal signature analysis

Osteoporosis can be defined as "a decrease in bone mass and strength leading to an increase in fracture" [1]. Although this definition requires fractures to have occurred before the condition is identified clinically, low bone density will have been present for some time. The need to identify those patients at risk of fracture has been helped by the development of a number of techniques for determining bone mineral density (BMD) [2, 3]. However, recent studies [4] have indicated that these measurements alone may be insufficient in determining the strength and solidity of cancellous bone, and that other techniques are needed to assess factors such as the trabecular architecture [5, 6] and to determine the relationship to the bone's mineral density and strength.

We report the results of a new method for quantifying the trabecular organization within human lumbar vertebrae. The detailed organization of the bone was recorded by high definition macroradiography [7, 8] and quantified using a recently developed method of fractal signature analysis (FSA) [9, 10]. The advantage of combining these two techniques is that the former records with unusually good resolution the fine detailed structural organization of cancellous bone, which is then quantified by FSA. Fractal analysis measures the degree of 'roughness' of an image of those structures, and also quantifies the change in roughness with alterations in spatial scale [11]. Self-similar images (looking the same at all magnifications) [12] are said to be 'fractal' and have associated with them a fractal dimension, between two and three for a surface [11]. When the pattern of a structure has altered at a particular size or sizes so as to be no longer self-similar, the 'fractal signature' of its image quantifies the alteration in the fractal dimension of the structure, and the size(s) at which those changes have occurred [9, 10]. The fractal dimension, and similarly the fractal signature, has no units as it is calculated from the ratio of two areas [11]. The fractal dimension of cancellous bone assesses the composite nature of the tissue, which is determined principally by trabecular number, spacing, and cross-connectivity [13], features referred to here as trabecular structures. The method of FSA provides more information than the mean fractal dimension employed by previous investigators [10, 11] which only quantifies the overall appearance of cancellous bone, whereas FSA measures separately the fractal dimension of the horizontal and vertical trabecular structures within the cancellous bone [9, 10] and quantifies how the fractal dimension varies with the size of the structures.

Our own [9, 10] and previous studies [14, 15] have shown that fractal analysis appears to be a robust method which is independent of a range of factors that are susceptible to variation during routine radiographic procedures: the effect of radiographic magnification and projection geometry [9, 10, 15], changes in object or patient position [9–15], and variations in the sensitometric properties of radiographs such as film contrast and mean density [9, 10, 15].

Two investigations were carried out in this study. The first was undertaken on postmortem lumbar vertebrae to assess the effect of superimposition of the neural arch on the FSA measure of cancellous bone organization within the vertebral body. In the second study, a comparison was made of the FSA obtained from the lumbar vertebrae between two groups of postmenopausal women, one with high and the other with low bone mineral density, to determine whether this method could detect differences in the trabecular orga-

Correspondence to: J. C. Buckland-Wright

Table 1. Details of the number of early postmenopausal women allocated to the groups with high and low BMD

	All patients (n = 47)			High BMD group (n = 28)			Low BMD group (n = 19)		
	Mean	SD	Range	Mean	SD	Range	Mean	SD	Range
Age (years)	54.1	3.2	42–60	53.6	3.5	42–58	54.9	2.5	49–60
Weight (kg)	65.6	11.2	47–99	65.8	10.6	47–92	65.5	12.2	48–99
Height (m)	1.61	0.07	1.47–1.77	1.60	0.07	1.50–1.75	1.62	0.08	1.47–1.77
BMI (kg m^{-2})	25.5	4.2	19.4–36.4	25.8	4.3	19.4–35.9	25.1	4.3	19.9–36.4
Time since last menstrual period (months)	53.3	9.5	31.0–71.0	54.5	8.6	38.0–71.0	51.6	10.7	31.0–70.0

Table shows the mean (SD) and range for the age, weight, body mass index (BMI), and time since last menstrual period

nization. Further, the FSA for horizontal and vertical trabecular structures was compared with the women's demographic data to determine whether any association existed between height, weight, body mass index (BMI), age, and vertebral BMD and the vertebral trabecular organization.

Materials and Methods

Experimental Procedure

Ten, clean and dry postmortem human lumbar vertebrae, with no obvious pathology, had high definition macroradiographs [7, 8], taken in the lateral and postero-anterior (P-A) views at ×4 magnification. The vertebrae were grouped in threes and held together in the anatomical position with an elastic band around the pedicles. The bodies of each vertebra were separated by foam pads in place of intervertebral discs. A 15-cm water bath was used as a soft tissue substitute. A steel ball (2 mm in diameter) was placed alongside the vertebrae for the accurate assessment of radiographic magnification. In addition, BMD measurements for each vertebral body were obtained by dual energy X-ray absorptiometry (DXA), using the Hologic QDA-1000.

Clinical Study Procedure

One hundred postmenopausal women were recruited who were between 6 and 36 months postmenopausal (as documented by time since last normal menstrual period and raised gonadotrophin levels). None had a history of metabolic bone disease, were taking drugs, or had coexistent diseases known to affect bone metabolism. All recruits were either nonsmokers or smoked less than 10 cigarettes/day. Women were excluded if they had had a hysterectomy or endometrial ablation. Informed consent was obtained from all women and the protocol was approved by the Guy's Hospital Ethical Committee.

Bone density measurements for each woman were obtained by DXA in the lumbar spine (L1–L4) using the Hologic QDA-1000. The precision error, based on repeat measures, was on average 1.1%. Height, weight, and age were obtained at the time of the scan. Postmenopausal women were allocated into two groups with high and low BMD. The women were ranked in order of their vertebral BMD from the highest to the lowest. The top and bottom 30 women in the list were invited into the study. Of these, 28 with high and 19 with low BMD attended and comprised the two groups studied, mean (SD) BMD values for the groups were 1.056 (0.119) and 0.854 (0.107) gm cm^{-2}. Details of the patients demographic data are given in Table 1.

A high definition macroradiograph [7, 8], at ×4 magnification, of the lumbar spine (L1-L4) was obtained in the P-A view for each patient (Fig. 1). Patients were secured within a stereotaxic unit to ensure that the spine was vertical and the body perpendicular to the X-ray beam. A steel ball (2 mm in diameter) was placed over the spine of L3 to allow the radiographic magnification to be measured.

Digitization of the Macroradiographs

The regions of interest selected for digitization in the macroradiographs of the postmortem vertebrae are shown in Figure 2. The area demarcated was digitized using a CCD camera (Videk Megaplus) linked via a frame grabber on a display board in an IBM PC-AT 80486 computer [9, 10]. By adjusting the camera to film distances, the effective pixel size was set to 0.06 mm (corresponding to 0.24 mm on the macroradiographs taken at ×4 magnification). The digital images were written to a SUN SPARCstation IPX (SUN Microsystems Ltd) and programs written in C were used to calculate the fractal signature [9, 10] for regions of interest in the images. As vertebral trabecular thickness and medullary space size in women is generally within 0.6–1.2 mm [16], the fractal signature calculations were carried out on data ranging from 1 to 20 pixels, corresponding to a scale of image feature sizes from 0.06 to 1.2 mm. In the P-A views of both the postmortem and patient vertebrae, the two regions of interest in each vertebra were combined (Fig. 2). For the patient study, the data from all the vertebrae, recorded in the macroradiograph (L1-L4), were combined and analyzed to give a single fractal signature for horizontal and vertical structures for each patient.

We assessed accuracy by determining the variations in measurements of FSA for horizontal and vertical structures from the macroradiograph of a vertebra redigitized six times, and for test-retest reliability by digitizing the macroradiographs of a vertebra repositioned and reradiographed six times. For the FSA of horizontal and vertical trabecular structures, the coefficients of variation were 0.87% and 0.89%, respectively.

Analysis of Experimental Data

The FSA for horizontal and vertical trabecular structure obtained from the lateral view of the vertebral body was compared with that obtained from the P-A view. The Wilcoxon matched pairs test was used to determine the difference in the FSA between the two radiographic views. The extent of the difference between the two views was assessed in relation to the coefficient of variation for errors of measurement and test-retest.

Pearson's correlation coefficient (R) and the nonparametric Kendall's tau-c test were used to assess the degree of association between the FSA for horizontal and vertical trabecular structures and the BMD values. The Kendall's tau-c test was used because of its greater power in determining the degree of association between parameters that may not have a strict linearity of fit [17].

Analysis of Clinical Data

Fractal signature analysis calculations, for each postmenopausal woman, were carried out blind as to whether they were from the high or low BMD group. Pearson's correlation coefficient (R) and the nonparametric Kendall's tau-c methods were used to assess the correlations between the FSA values for the horizontal and vertical trabecular structures and the patients' demographic data for height, weight, BMI, age, and vertebral BMD. The BMI was calculated using the formula: body weight kg/[height (m)]^2 [18].

Differences in fractal signature values, for horizontal and vertical trabecular structures, between the high and low BMD groups were examined using the Mann-Whitney test. Differences between the fractal signatures for horizontal and vertical structures were analyzed using the Wilcoxon matched pairs test.

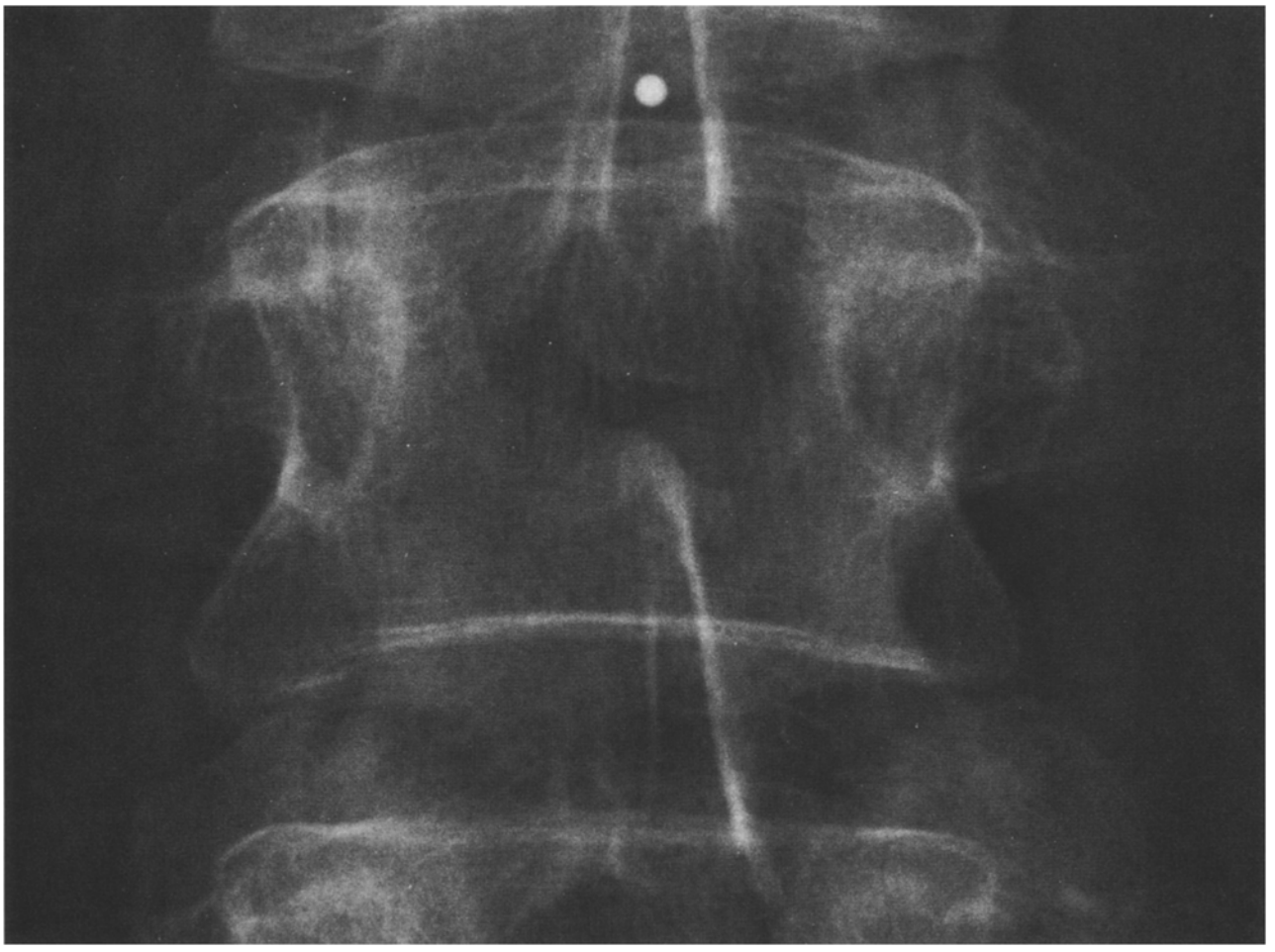

Fig. 1. Third lumbar vertebrae from part of a macroradiograph of the spine. Original magnification ×4, reproduced at ×2.25.

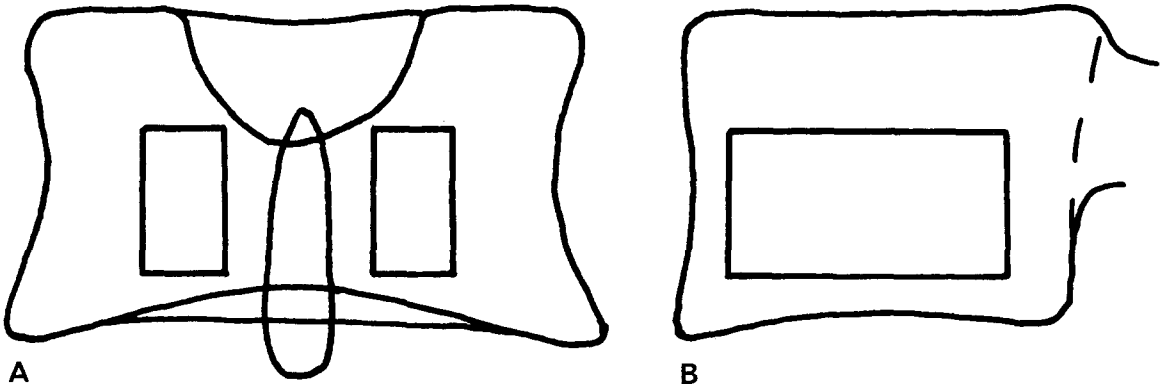

Fig. 2. Diagrams of the P-A (**A**) and lateral (**B**) radiographic views of the lumbar vertebrae, illustrating the regions of interest located within the same horizontal plane of the vertebra, selected for fractal signature analysis of the trabecular organization.

Results

Experimental Data

No significant difference was found in the FSA for vertical and horizontal trabecular structures between vertebrae radiographed in the lateral and in the P-A planes (Fig. 3). Any differences in the fractal signature between the two views were within two SDs of the coefficient of variation for errors of measurement and test-retest. These findings indicate that in the P-A view of the vertebrae, the presence of trabecular structures within the neural arch did not affect the FSA

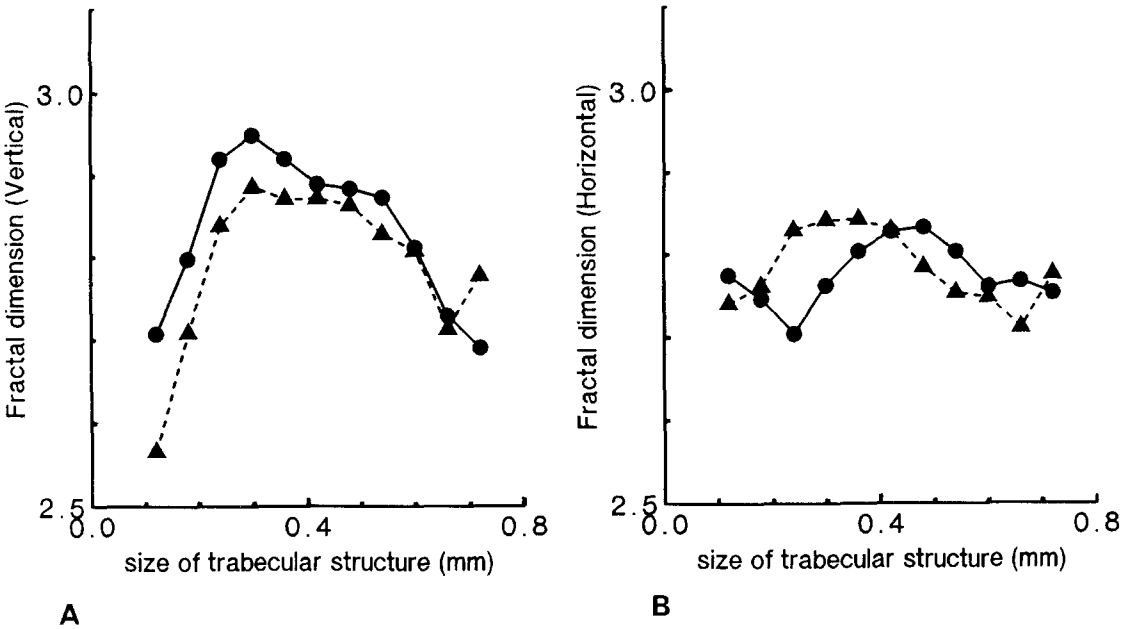

Fig. 3. Fractal signatures for (**A**) vertical and (**B**) horizontal trabecular structures within a postmortem lumbar vertebra, showing no difference in the signature obtained from either the P-A (▲) and lateral (●) radiographic planes.

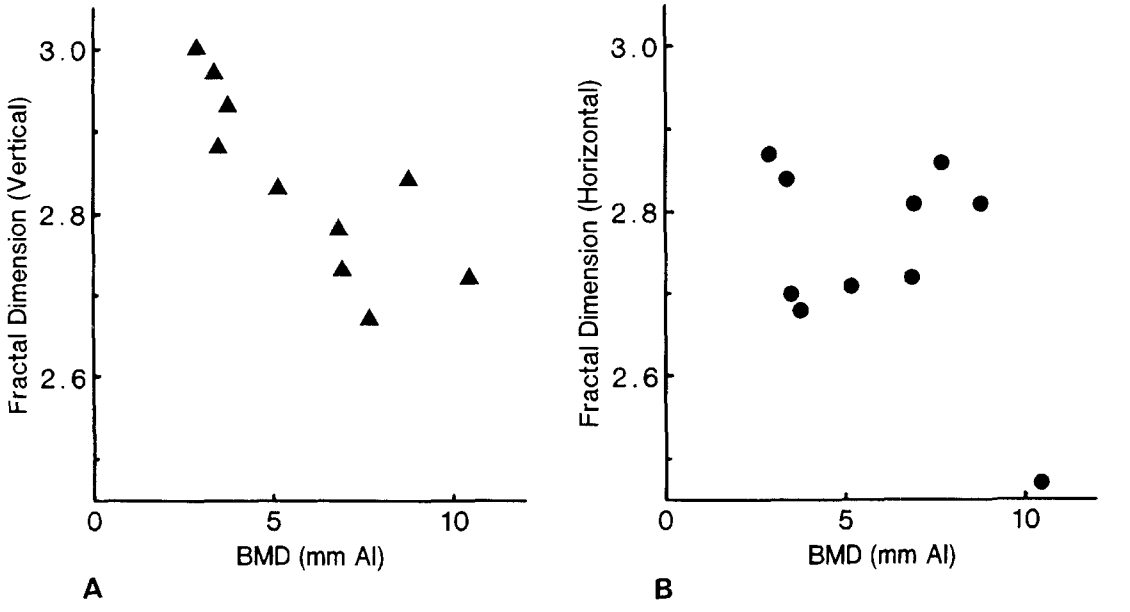

Fig. 4. Comparison of the overall fractal dimension with bone mineral density (BMD) showed an inverse correlation with vertical (**A**) and no correlation with the horizontal (**B**) trabecular structures, in the 10 postmortem vertebrae.

assessment of trabecular organization within the vertebral body. In addition, the results showed that a difference in the radiographic angle of view as great as ±90° had no significant effect on the estimate of the fractal signature for either horizontal or vertical trabecular structures.

Vertebral BMD was found to correlate inversely with the FSA for vertical trabecular structures (Fig. 4), between the image feature sizes of 0.18–0.90 mm (Pearson R −0.66, tau c −0.42, giving $P < 0.04$). No correlation was found between the FSA for horizontal trabecular structures and BMD measurements (Fig. 4).

Clinical Data

In the group of postmenopausal women as a whole, vertebral BMD correlated inversely with the FSA values for the image of the fine vertical trabecular structure (ranging in size from 0.12 to 0.42 mm) (Tables 1 & 2). The women's weight and BMI correlated with the FSA values for coarse vertical trabecular structures only (for weight: image features ranging in size from 0.48 to 1.08 mm; and BMI: ranging in size from 0.42 to 1.14 mm) (Tables 1 and 2). The women's age correlated with the FSA values for the image of the fine horizontal

Table 2. Mean (SD) fractal signatures for vertical and horizontal trabecular structures and the significance of correlations calculated using Kendall's τ_c between fractal signatures and spinal BMD, patient weight, BMI, and patient age

Image feature size (mm)	Mean (SD) fractal signatures		Significance of correlation with fractal signatures			
	Vertical trabecular structures	Horizontal trabecular structures	Vertical trabecular structures		Horizontal trabecular structures	
			BMD	Weight	BMI	Age
0.12	2.71 (0.07)	2.80 (0.07)	0.05			0.02
0.18	2.69 (0.07)	2.72 (0.08)	0.03			0.005
0.24	2.71 (0.09)	2.69 (0.09)	0.007			0.05
0.30	2.69 (0.10)	2.67 (0.09)	0.005			
0.36	2.67 (0.12)	2.65 (0.12)	0.008			
0.42	2.67 (0.12)	2.63 (0.12)	0.04		0.05	
0.48	2.67 (0.13)	2.62 (0.12)		0.02	0.005	
0.54	2.67 (0.14)	2.62 (0.12)		0.02	0.007	
0.60	2.69 (0.14)	2.63 (0.13)	0.04	0.02	0.02	
0.66	2.70 (0.15)	2.65 (0.15)		0.01	0.02	
0.72	2.71 (0.17)	2.66 (0.15)		0.02	0.02	
0.78	2.73 (0.18)	2.67 (0.16)		0.03	0.03	
0.84	2.77 (0.20)	2.69 (0.16)		0.03		
0.90	2.82 (0.21)	2.71 (0.18)		0.02	0.03	
0.96	2.89 (0.25)	2.75 (0.21)		0.01	0.009	
1.02	2.91 (0.26)	2.80 (0.26)		0.03	0.009	
1.08	2.94 (0.27)	2.83 (0.27)		0.03	0.02	
1.14	3.01 (0.31)	2.87 (0.32)			0.02	

Nonsignificant correlations ($P > 0.05$) are not shown, and significant correlations were positive except for that between fractal signature and BMD which is an inverse correlation

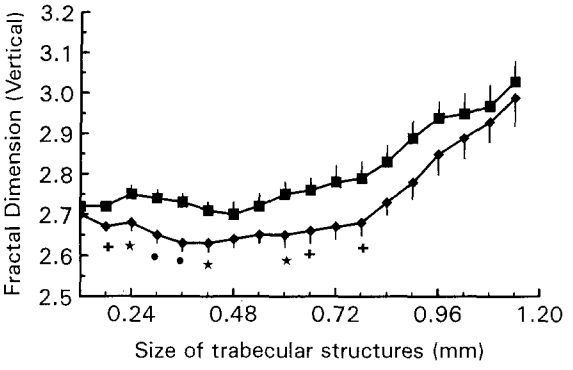

Fig. 5. The mean (SE) fractal signature for vertical trabecular structures was greater in early postmenopausal women with low (■) compared with those with high (♦) bone mineral densities. The significance of difference in the vertical structures between the two groups is indicated by the symbols under the signature for the high BMD group: ● = $P < 0.0025$, ★ = $P < 0.025$, + = $P < 0.04$.

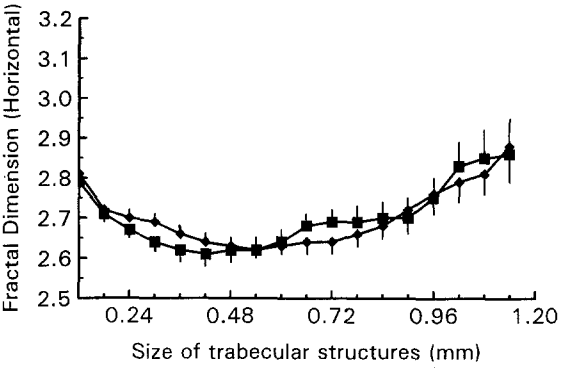

Fig. 6. The mean (SE) fractal signature for horizontal trabecular structures was similar in early postmenopausal women with low (■) and high (♦) bone mineral densities.

trabecular structures (ranging in size from 0.12 to 0.24 mm) (Tables 1 and 2). No correlation was found between the women's height and the fractal signature for either horizontal or vertical trabecular structures.

Figures 5 and 6 show the FSA for the radiographic image of horizontal and vertical trabecular structures in the vertebrae of postmenopausal women with high and low BMD. In the women from the latter group, the FSA for the image of the vertical structures had increased above that recorded in the women's vertebrae from the high BMD group (Fig. 5). This difference in the FSA between the two groups reached significance in the vertical trabecular structures with image features ranging in size from 0.18 to 0.42 mm, with the greatest difference at sizes from 0.30 to 0.36 mm (Fig. 5). No difference was found in the FSA for horizontal trabecular structures between the high and low BMD groups (Fig 6).

Discussion

Further evidence of the robustness of the FSA technique [9–15] was provided in this study by the low coefficient of variation for the method of fractal signature measurement, and its independence from both variations in the radiographic angle of projection within the transverse plane of the body, and of the effect of superimposition of the neural arch. Thus, FSA of the vertebral cancellous bone can be obtained equally from radiographs taken in the postero-anterior as from the lateral view. In our studies, the P-A view was adopted because it resulted in a lower radiation dose to the patient, and a concordance between the data obtained from the macroradiographic and densitometric methods not ob-

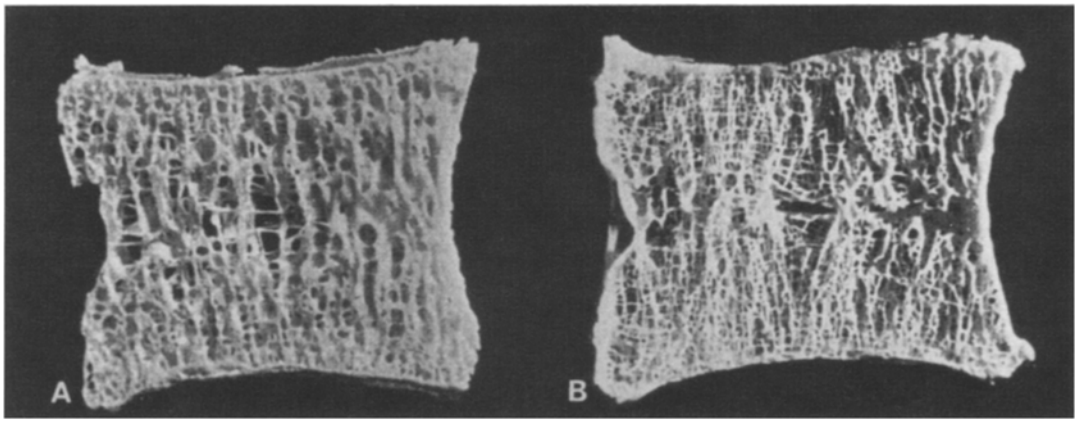

Fig. 7. Macerated preparations of lumbar vertebrae showing differences in the trabecular organization of vertebrae from subjects with 'normal' structure (**A**) and mild osteoporosis (**B**). The appearance of 'roughness' in the trabecular structure of (**B**) is greater than in (**A**) due to the larger number of trabeculae visible, resulting from narrowing of the trabecular plates visible in (**A**). (Reproduced with permission from Remagen [24].)

tained from the lateral projection. In addition, the results indicated that the laminae either possessed few trabeculae and/or had a trabecular structure of similar dimensions to that within the vertebral body.

In the postmenopausal women, FSA of the trabecular organization recorded in the macroradiographs of the lumbar spine showed that the coarse vertical trabecular structures, with an image size ranging from a half to over 1 mm, correlated significantly with both women's overall weight and BMI (Tables 1 & 2), conforming to the expected association between bone and load transmission [19–21]. No similar relationship was found between BMD and the coarse vertical trabecular structures. Instead, BMD correlated inversely with the fine vertical trabecular structures not only in the postmenopausal women (Tables 1 & 2), but also in the group of postmortem vertebrae. Under these circumstances, bone mineral loss would appear to correspond to the description of the early stages of axial bone loss in postmenopausal women [19]. This process begins with the focal perforation of coarse vertical trabecular plates and progresses by converting these fenestrated plates into a lattice of bars and rods [19]. These changes would result in an increase in the number and cross-connectivity of fine trabecular structures and a higher fractal signature value due to the increased appearance of 'roughness' of the trabecular organization. The difference between this pattern of trabecular organization and that in 'normal,' healthy vertebrae is illustrated in the sections of macerated vertebrae in Figure 7.

Further, the women's age correlated directly with the FSA regarding the very fine horizontal trabecular structures recorded in the macroradiographs of the vertebrae. Age-related changes in the vertebral cancellous bone detected by conventional radiography have been described as a reduction in the number of horizontal trabeculae [16, 19, 22, 23]. The high spatial resolution (<50 μm) and primary magnification obtained with microfocal radiography have made it possible to show that within the age range of the women (40–60 years), very fine horizontal trabeculae, not detected by conventional radiography, were more numerous in older than the younger women. Comparison of the FSA obtained from the group of postmenopausal women with high and low BMD showed that the increase in the fine vertical structures correlated with decreased bone density.

Although the present results are encouraging, further studies are still required to provide more information on the precise relationship between FSA of the macroradiographic image and the structural organization of the cancellous bone.

Acknowledgments. We would like to thank Judy Vlahovic for her help in X-raying the patients and postmortem samples, Liz Johnson for her analysis of the postmortem vertebrae, which formed part of a project submitted for her BSc degree, and Kevin Fitzpatrick and Sarah Smith for photographic assistance.

References

1. Riggs BL, Melton LJ (1992) The prevention and treatment of osteoporosis. N Engl J Med 327:620–627
2. Fogelman I, Rodin A, Blake G (1990) Impact of bone mineral measurements on osteoporosis. Eur J Nucl Med 16:39–52
3. Genant HK, Faulkner KG, Gluer C-C (1991) Measurement of bone mineral density: current status. Am J Med 91(suppl 5B): 49S–53S
4. Wallach S, Feinblatt JD, Avioli LV (1992) The bone quality problem. Calcif Tissue Int 51:169–172
5. Chevalier F, Laval-Jeantet AM, Laval-Jeantet M, Bergot C (1992) CT image analysis of the vertebral trabecular network in vivo. Calcif Tissue Int 51:8–13
6. Caligiuri P, Giger M, Favus MJ, Jia H, Doi K, Dixon LB (1993) Computerised radiographic analysis of osteoporosis: preliminary evaluation. Radiol 186:471–474
7. Buckland-Wright JC (1989) A new high definition microfocal X-ray unit. Br J Radiol 62:201–208
8. Buckland-Wright JC, Bradshaw CR (1989) Clinical applications of high-definition microfocal radiography. Br J Radiol 62:209–217
9. Lynch JA, Hawkes DJ, Buckland-Wright JC (1991) Analysis of texture in macroradiographs of osteoarthritic knees using the fractal signature. Phys Med Biol 36:709–722
10. Lynch JA, Hawkes DJ, Buckland-Wright JC (1991) A robust and accurate method for calculating the fractal signature of texture in macroradiographs of osteoarthritic knees. Med Inform 16:241–251
11. Pentland AP (1984) Fractal based descriptions of natural scenes. IEEE Trans Pattern Ann Machine Intell PAMI-6:661–674
12. Feder J (1988) Fractals. New York, Plenum Press
13. Majumdar S, Weistein RS, Prased RR, Genant HK (1993) The fractal dimension of trabecular bone: a measure of trabecular structure. Calcif Tissue Int 52:168

14. Lundahl T, Ohley WS, Kay SM, Siffert R (1986) Fractional Brownian-motion: a maximum likelihood estimator and its application to imaging texture. IEEE Trans Med Imaging MI-5: 152–161
15. Ruttiman UE, Webber RL, Hazelrig JB (1992) Fractal dimension from radiographs of periodontal alveolar bone. A possible diagnostic indicator of osteoporosis. Oral Surg Oral Med Pathol 74:98–110
16. Bergot C, Laval-Jeantet AM, Preteux F, Meunier A (1988) Measurement of anisotropic vertebral trabecular bone loss during aging by quantitative image analysis. Calcif Tissue Int 43:143–149
17. Campbell MJ, Machin D (1990) Medical statistics: a commonsense approach. John Wiley, New York
18. Lentner C (1984) Geigy scientific tables vol. 3, 8th ed. Ciba Geigy Ltd, Basle, p 327
19. Parfitt AM (1987) Trabecular bone architecture in the pathogenesis and prevention of fracture. Am J Med 82 (suppl 1B):68–72
20. Martin RB (1991) Determinants of the mechanical properties of bone. J Biomech 24:79–88
21. Gibson LJ (1985) The mechanical behaviour of cancellous bone. J Biochem 18:317–328
22. Atkinson PJ (1967) Variation of trabecular structure of vertebrae with age. Calcif Tissue Res 1:24–32
23. Mosekilde L (1988) Age related changes in vertebral trabecular bone architecture—assessed by a new method. Bone 9:247–250
24. Remagen W (1989) Osteoporosis. Sandoz Ltd, Basle, p 33